Journal of Membrane Science 643 (2022) 120047

Contents lists available at ScienceDirect

Journal of Membrane Science

journal homepage: www.elsevier.com/locate/memsci

Design and optimization of Single Pass Tangential Flow Filtration for inline concentration of monoclonal antibodies

Mario G. Jabra, Andrew L. Zydney *

Department of Chemical Engineering, The Pennsylvania State University, University Park, PA, 16802, USA

ARTICLE INFO

Keywords:
SPTFF
Ultrafiltration
Diafiltration
Antibody
Continuous processing

ABSTRACT

A number of Single Pass Tangential Flow Filtration (SPTFF) systems have recently been commercialized for inline concentration of monoclonal antibodies and other biotherapeutics, both to resolve bottlenecks in existing processes and as part of the development of integrated continuous downstream processes. The objective of this study was to examine the design and optimization of SPTFF modules using a previously developed mathematical model for the filtrate flux and pressure drop that specifically accounts for the concentration dependence of the antibody viscosity and osmotic pressure as well as the variation of the flow rate and antibody concentration with the position in the long pathlength SPTFF device. Model simulations were performed to examine the effects of channel width, length, and cassette staging (number of parallel cassettes in each stage) on SPTFF performance. The concentration factor (conversion) was greatest for a long thin channel configuration, but this also caused very large feed-side pressure drops. The use of cascade configurations, with a greater number of parallel channels near the feed inlet, significantly reduced the pressure drop but with a corresponding increase in total membrane area. A key factor governing the SPTFF performance was the increase in viscosity of the antibody solution at high conversion. These results provide important insights into the design and optimization of SPTFF systems for monoclonal antibody processing.

1. Introduction

There is considerable interest in the application of Single Pass Tangential Flow Filtration (SPTFF), both for intensification of (existing) batch processes and for the development of new continuous downstream processes for the production of monoclonal antibodies (mAbs) and other biotherapeutics. For example, Dizon-Maspat et al. [1] explored the use of SPTFF for the inline reduction of process intermediate volumes, with the results demonstrating that SPTFF could help accommodate an increase in protein titer (mass throughput) using existing stainless steel tanks in a commercial manufacturing facility. Elich et al. [2] showed that SPTFF could be used to improve the performance of an anion exchange chromatography step, with the preconcentrated feed showing an improved binding isotherm leading to a 4-fold increase in antibody loading at the same level of host cell protein removal. Brinkmann et al. [3] used SPTFF to reduce the harvest volume from a fed-batch bioreactor, with the more concentrated feed stream providing a 5-fold increase in the productivity of the subsequent Protein A capture step. Perry and Rayat [4] discussed the potential application of SPTFF for enhanced production of lentiviral vectors for gene processing, although no experimental results were presented.

SPTFF can also be used for final concentration and formulation. Casey et al. [5] used SPTFF for final concentration of an IgG feed solution, increasing the IgG concentration from 45 g/L to approximately 200 g/L in a single pass. Rucker-Pezzini et al. [6] used a series of sequential dilution and concentration (SPTFF) steps for buffer exchange, with 99.75% removal of a trace impurity from a mAb. Nambiar et al. [7] demonstrated that countercurrent staging of SPTFF modules could provide more effective buffer exchange by effectively "re-using" the diafiltration buffer between stages. This approach was subsequently extended by Jabra et al. [8], with a 3-stage countercurrent system providing >99.9% removal of a small impurity over 24 h of continuous operation.

Several groups have developed models for SPTFF performance to aid in the development of SPTFF processes. For example, Huter and Strube [9] developed an SPTFF model that accounted for the underlying fluid dynamics and concentration polarization effects, but the analysis did not explicitly account for the variation in flow rate and concentration in the

* Corresponding author. Department of Chemical Engineering, The Pennsylvania State University, 404 Chemical & Biomedical Engineering Building, University Park, PA, 16802, USA.
E-mail address: zydney@engr.psu.edu (A.L. Zydney).

https://doi.org/10.1016/j.memsci.2021.120047
Received 24 September 2021; Received in revised form 31 October 2021; Accepted 4 November 2021
Available online 9 November 2021

long path-length SPTFF modules. Thakur and Rathore [10] specifically examined the effects of different module configurations (series and parallel arrangements), but the filtrate flux was evaluated using a largely empirical model for the protein deposition kinetics, making it difficult to extrapolate their results to other systems/geometries.

Several different approaches have been used to develop commercial SPTFF modules for bioprocessing applications. The pioneering work by de los Reyes and Mir [11] used a cascade arrangement of tangential flow filtration channels, with the number of parallel channels decreasing as one moves from the feed inlet to the retentate exit to increase the local shear rate, and thus the filtrate flux, even as the retentate flow rate decreases. Pall Corporation has commercialized a number of SPTFF modules based on this technology, ranging from a 4-in-series configuration (with 3 cassettes followed by 2 then 1 and 1) to a 9-in-series module that uses a total of 21 channels [12]. In contrast, MilliporeSigma sells the Pellicon® SPTFF system that uses conventional UF modules arranged in series to obtain a longer effective channel length but without any change in the number of parallel channels (or effective membrane width) within the system [13]. Yehl and Zydney [14] took a very different approach, using low-cost hollow fiber modules that were only 26 cm long but operated at sufficiently low feed flow rates to achieve more than a 10-fold concentration in a single pass.

The diversity of SPTFF configurations is due, at least in part, to the lack of detailed understanding of the key factors that govern the performance of these SPTFF modules for specific applications. The objective of this study was to examine the design and optimization of SPTFF modules using the mathematical model recently developed by Jabra et al. [15] that accounts for the variation in both flow rate and mAb concentration with position due to the high conversion in these modules. A number of module geometries are explored, including the effects of module width/length as well as different cascade configurations. These results provide important insights into the development and optimization of SPTFF modules for specific target applications in bioprocessing.

2. SPTFF model development

The performance of the SPTFF module was described using the model developed previously by Jabra et al. [15] that accounts for both the variation in flow rate/protein concentration due to removal of permeate as well as the effects of protein-protein interactions on the filtrate flux through the concentration dependence of the protein viscosity and osmotic pressure. The resulting equations involve no adjustable parameters (i.e., there are no parameters that must be fit to the filtrate flux data). This is in contrast to the models developed by Huter and Strube [9] and Huter et al. [16] in which the boundary layer resistance must be fit to data for the measured filtrate flux in the specific SPTFF module, making it unclear whether these equations can be directly extended to other module geometries. Similarly, Krippl et al. [17] developed a hybrid model for SPTFF incorporating a machine learning approach, although significant care would need to be taken in the extrapolation of this modeling approach outside the range of modules on which the system was trained.

The local filtrate flux was evaluated by interpolation between the membrane-limited (J_{mem}) and mass transfer limited filtrate flux (J_{lim}):

$$\frac{1}{J_v}=\frac{1}{J_{lim}}+\frac{1}{J_{mem}} \tag{1}$$

The local value of J_{lim} was evaluated in terms of the local bulk protein concentration (C_b) using the model equation presented by Binabaji et al. [18]:

$$J_{lim}=k_0\left(\frac{\eta_b}{\eta_0}\right)^{\frac{1}{3}}\int_{C_b}^{C_w}\left(\frac{M_p}{RT}\right)\left(\frac{\eta_0}{\eta}\right)\left(\frac{d\Pi}{dC}\right)\frac{dC}{C} \tag{2}$$

where C, C_w, and C_b are the local, wall, and bulk protein concentrations; η, η_o, and η_b are the local, solvent, and bulk viscosities; and M_p is the protein molecular weight. Note that the paper by Jabra et al. [15] has an error in the exponent on η_b/η_o that was subsequently corrected [19]. k_0 is the local mass transfer coefficient, which can be evaluated as a function of the local retentate flow rate using the Sherwood number correlation presented by Da Costa et al. [20]:

$$Sh=\frac{k_o d_h}{D_p}=0.664Re^{0.5}Sc^{0.33}\left(\frac{d_h}{l_m}\right)^{0.5} \tag{3}$$

where $Re=\frac{Ud_h}{\nu}$ is the local Reynold number, $Sc=\frac{\nu}{D_p}$ is the local Schmidt number, U is the local velocity, d_h and l_m are the hydraulic diameter and mesh length, respectively, and ν is the kinematic viscosity. The membrane-limited flux was evaluated simply as the product of the effective pressure driving force (equal to the difference between the local transmembrane and osmotic pressures (ΔP_{TM} - $\Delta\pi$) and the membrane permeability (L_p).

The variations in the retentate flow rate (Q), protein concentration (C), and pressure (P) along the length (z) of the module were evaluated using overall mass and momentum balances:

$$\frac{dQ}{dz}=-2NwJ_v \tag{4}$$

$$\frac{d(QC)}{dz}=-2NwCS_oJ_v \tag{5}$$

$$\frac{dP}{dz}=-\frac{\beta}{N}\eta Q \tag{6}$$

where N and w are the number and width of the channels in each stage of the module, S_o is the protein sieving coefficient, and β is a geometric factor describing the parasitic pressure losses due to flow through the screened channel. All simulations presented in this work were for fully retentive membranes ($S_o = 0$); thus, the right-hand side of Equation (5) was set equal to zero. Note that Equation (6) neglects the pressure loss in the manifold that connects individual channels (or cassettes) in many SPTFF modules. Equations (4) and (5) can also be applied to hollow fiber modules with w replaced by πR where R is the fiber radius. Additional details on the model equations are provided elsewhere [15]. The governing ordinary differential equations were integrated numerically in Mathematica version 12 (Wolfram).

Most of the model calculations were performed using modules having similar properties to those of commercially available Pellicon® 3 cassettes with Ultracel 30 kDa membranes and C screen (MilliporeSigma, Bedford, MA) which have a mesh length of 500 μm and hydraulic diameter of 100 μm [13]. Model simulations were focused on exploring the effects of membrane geometry (length and width), total membrane area (A), and device configuration (internal staging) on the SPTFF performance, including the concentration factor (X = ratio of exit to inlet mAb concentrations) and the feed-side pressure drop (ΔP). Fig. 1 provides a schematic of some of the module configurations that were examined. The notation 3-2-1 denotes a device in which there are 3 cassettes in parallel in the first "stage" followed by a region with 2 cassettes in parallel and then only a single cassette near the device exit. The parallel arrangement increases the effective membrane width, shown in Fig. 1 by an increase in the number of parallel channels that divide the flow. This could also be accomplished by an actual increase in width or by placing the channels next to each other. In contrast, the series arrangement increases the overall length of the channel.

3. Results and discussion

Fig. 2 shows results for the concentration factor and feed-side pressure drop for 1, 2, 3, and 4 Pellicon® 3 cassettes in series (corresponding to total lengths of L = 20, 40, 60, and 80 cm) at different feed flow rates for $C_F = 20$ g/L. The width of each Pellicon® 3 cassette is 2.2 cm giving a

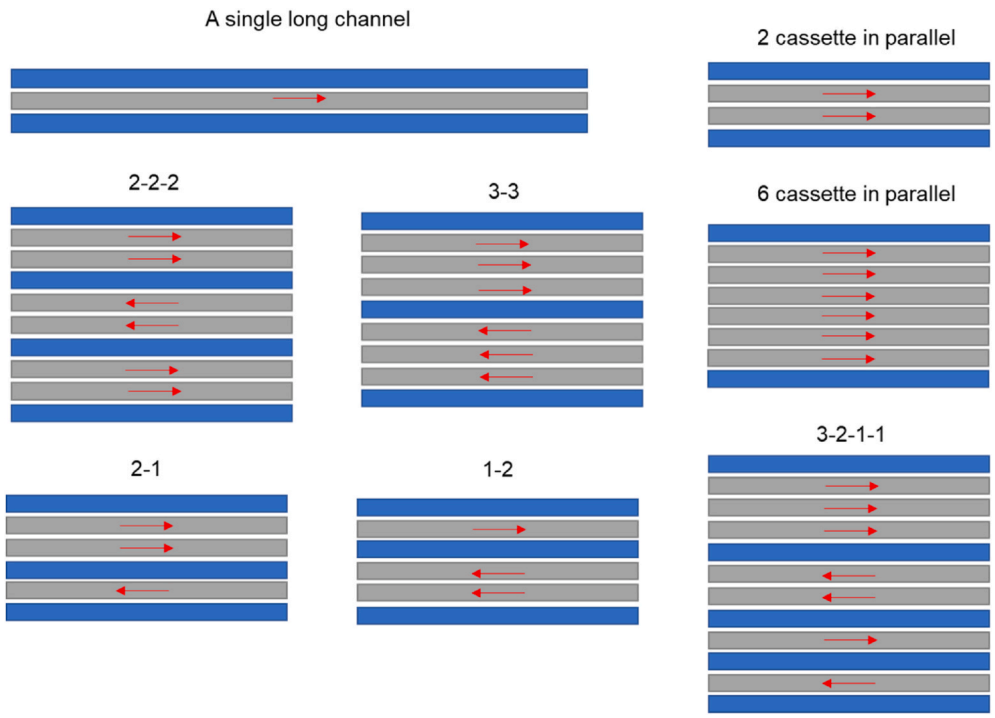

Fig. 1. Diagram showing a schematic of various module configurations (cassette arrangements) for the SPTFF system. Devices are not drawn to scale.

total area of 88 cm^2 per cassette (A = 2wL since the channel has an upper and lower membrane). In each case, the model calculations were performed with P_F = 310 kPa (45 psi), with the governing equations integrated along the channel length until z = L. Also shown for comparison are experimental data for systems with 1 and 2 cassettes in series from Jabra et al. [15]; the experimental values are in good agreement with the model calculations for both the concentration factor and pressure drop. Note that the experimental data were obtained at a mean transmembrane pressure of 50 kPa, which is in the mass transfer-limited regime where the filtrate flux, and thus the concentration factor, are essentially independent of both the transmembrane pressure and the membrane permeability. It was not possible to obtain data for the 3- and 4-in series configurations due to the lack of available Pellicon® 3 cassettes.

The concentration factor decreases with increasing feed flow rate since the mass transfer coefficient varies with Reynolds number to the ½ power. Thus, a doubling of the feed flow rate will provide only about a 40% increase in the mass transfer-limited flux (and an even smaller change in the membrane-limited flux). The concentration factor also increases with increasing channel length due to the increase in membrane area. The concentration factors become greater than X = 5 for feed flow rates below 7 mL/min at L = 80 cm and below 1 mL/min at L = 20 cm. It is worth noting that the recommended feed fluxes (feed flow rate normalized by the membrane area) for the Pellicon® 3 cassettes are between 240 and 360 L/m^2/h which is equivalent to a feed flow rate between 35 and 53 mL/min for N = 1 and between 140 and 210 mL/min for N = 4. However, these high feed flow rates provide relatively low conversion, requiring continued recirculation of the feed through the module as is typical in batch ultrafiltration processes.

The behavior of the feed side pressure drop is more complex (bottom panel of Fig. 2). The pressure varies nearly linearly with Q_F at high feed flow rates, reflecting the small concentration factors under these conditions (top panel), which leads to a nearly constant retentate flow rate throughout the module. The increase in pressure drop at very low feed flow rates is a direct result of the large increase in viscosity of the concentrated mAb solution that is generated under these conditions due to the high conversion (large X) in the SPTFF module. Model calculations using the correlation developed for the viscosity of the mAb solution show that the product η*Q increases at very low flow rates (see Supplementary Information). This effect is most pronounced for the module with 4 cassettes in series (L = 80 cm) since the conversion and thus the mAb viscosity are greatest under these conditions. For example, at a flow rate of 5 mL/min, the concentration factor for the 4 cassettes is around X = 7 giving a mAb concentration of 140 g/L near the retentate exit, corresponding to more than an 11-fold increase in viscosity.

To understand the pressure drop behavior in more detail, the results in Fig. 2 were replotted as the scaled pressure drop $\Delta P/\Delta P_0$, where ΔP_0 is the pressure drop through the module evaluated assuming that the flow rate and viscosity are both constant at their exit values:

$$\Delta P_0 = -\frac{\beta}{N}\eta Q L \tag{7}$$

This scaling highlights the effects of the conversion and module geometry on the pressure drop behavior given the importance of the high viscosity at the module exit in determining the pressure drop. The results for the different module lengths tend to collapse to a single curve when plotted as the scaled pressure drop as a function of the mAb concentration at the device exit (C_R). The scaled pressure drop initially increases with increasing feed flow rate since the reduction in Q is more significant than the increase in viscosity at low mAb concentrations. The scaled pressure drop goes through a maximum around 50 g/L and then decreases at high exit concentrations due to the very high viscosity at the high mAb concentrations (η varies exponentially with C).

The effect of channel width and length on the performance of the SPTFF process was examined by performing calculations for a system with six cassettes, each 20 cm in length and 2 cm in width, arranged in different series and parallel configurations: (a) 6 channels in parallel (corresponding to a single 20 cm long channel with a total width of 12 cm), (b) 3 channels in parallel followed by a second 3 channels in parallel (corresponding to a single channel with a total length of 40 cm and a total width of 6 cm), (c) a 2-2-2 configuration (L = 60 cm and w = 4 cm), and (d) all 6 single channels in series giving a 1-1-1-1-1-1 configuration (L = 120 cm). All four configurations had the same total membrane area of A = 2wL = 480 cm^2. Note that this is less area than 6

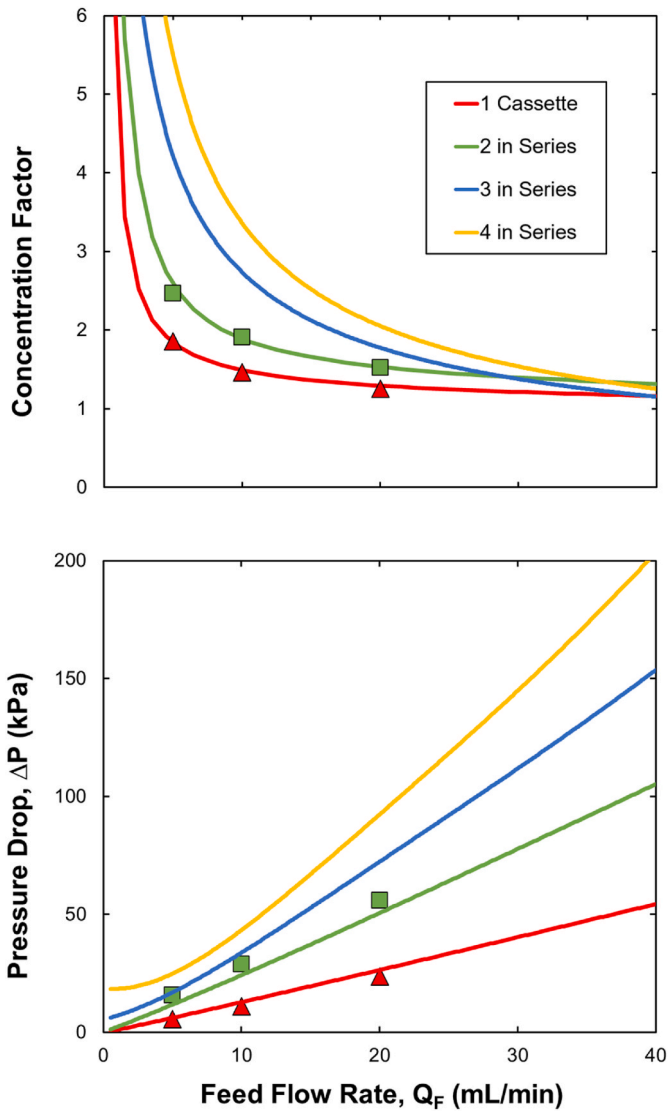

Fig. 2. Concentration factor (top panel) and feed-side pressure drop (bottom panel) as a function of the feed flow rate for different numbers of Pellicon® 3 cassettes in series (L_{total} = 20–80 cm with w = 2.2 cm) at a mean transmembrane pressure of 50 kPa and C_F = 20 g/L. Experimental data for 1 and 2 cassettes in series are from Jabra et al. [15] at a mean transmembrane pressure of 50 kPa.

Pellicon® 3 cassettes since the calculations were performed using w = 2 cm instead of the 2.2 cm in the Pellicon® 3. Simulations were performed over a range of feed flow rates with C_F = 10 g/L; similar results were obtained at other mAb concentrations, with the concentration factor decreasing with increasing C_F while the pressure drop increases. As shown in Fig. 4, the concentration factor was greatest for the configuration with all 6 cassettes in series (L = 120 cm), which has the highest mass transfer coefficient due to the large Reynolds number (Equation (3)). However, this configuration also has the largest pressure drop due to the very long channel length and high feed velocity, with ΔP = 98 kPa at a feed flow rate of 20 mL/min compared to only 3 kPa for the fully parallel arrangement (L = 20 cm). The minimum pressure drop in the series configuration occurs at Q_F = 13.5 mL/min; operation at lower feed flow rates leads to a greater pressure drop due to the increase in viscosity that occurs at high conversion. The concentration factor decreases as one moves to a more highly parallel arrangement due to the reduction in the mass transfer coefficient caused by the lower Reynolds number. In addition, the minimum in the pressure drop shifts to smaller

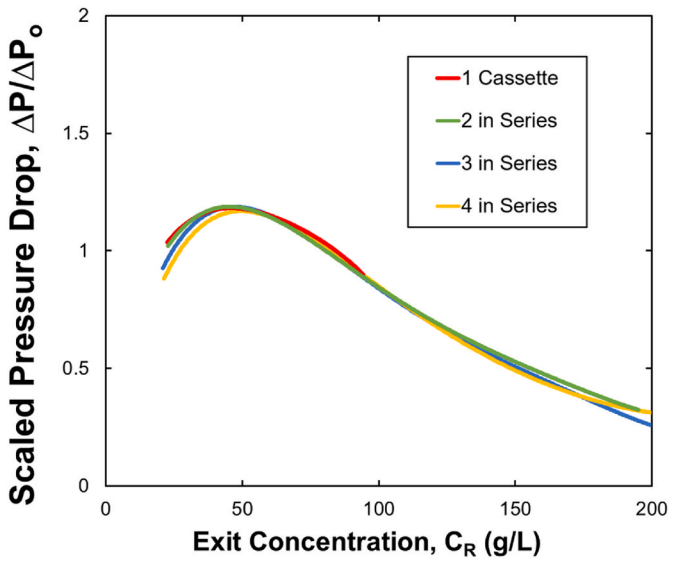

Fig. 3. Plot of the dimensionless pressure drop versus the final retentate concentration at C_F = 20 g/L for different numbers of modules in series.

Q_F due to the corresponding reduction in the conversion. The pressure drop data for the different configurations again tend to collapse to a single curve when plotted as in Fig. 3 (results not shown).

In addition to the channel configurations examined in Fig. 4, it is also possible to arrange the six channels in tapered configurations, e.g., with 3 parallel channels followed by 2 parallel channels and then 1 channel, which we label as the 3-2-1 configuration (shown schematically in Fig. 1). The concentration factor and pressure drop for several possible arrangements of the 6 cassettes are summarized in Fig. 5 for a feed concentration of 10 g/L, a feed flow rate of 20 mL/min, and a feed pressure of 310 kPa. The concentration factor is determined primarily by the total length of the SPTFF module, with the concentration factor decreasing from X = 14.5 for the 1-1-1-1-1-1 configuration (L = 120 cm) to X = 6.9 ± 0.2 for the 3 configurations with L = 60 cm (3-2-1, 2-2-2, and 1-2-3), to X = 4.5 ± 0.1 for the 3 configurations with L = 40 cm, and finally to X = 2.7 for the fully parallel arrangement with L = 20 cm. For configurations with the same total length, the concentration factor is largest for the more uniform arrangement, e.g., 2-2-2 has a slightly greater concentration factor than either the 3-2-1 or 1-2-3 configurations, since the uniform arrangement eliminates having a region with very low Reynolds. This behavior is only valid when the filtrate flux is mass transfer limited. The use of very low pressures, or very high flow rates, tends to reduce the dependence on the detailed module configuration, with the concentration factor becoming dependent only on the total membrane area during operation in the membrane-limited regime.

The pressure drop also tends to scale with the total channel length, but in this case, there are significant differences between the different configurations with the same total channel length. For example, the pressure drop for the 3-2-1 cascade is only 2.5 kPa; this increases by more than 40% to 3.6 kPa for the 1-2-3 configuration. The lower pressure drop for the 3-2-1 configuration is due to the more uniform flow distribution per module with this arrangement; the high inlet feed flow rate is split among more parallel channels while the lower flow rate near the device exit is handled in a single channel. This effect would be even more pronounced if operating the module at higher feed concentrations, with the latter due to the increase in viscosity of the mAb solution. The pressure drop becomes largely independent of the module configuration when operating at low conversion since the feed-side flow rate becomes nearly independent of position under these conditions. This behavior also depends on the details of the viscosity correlation (see Supplementary Information).

The analysis in Fig. 5 examined the performance of the different

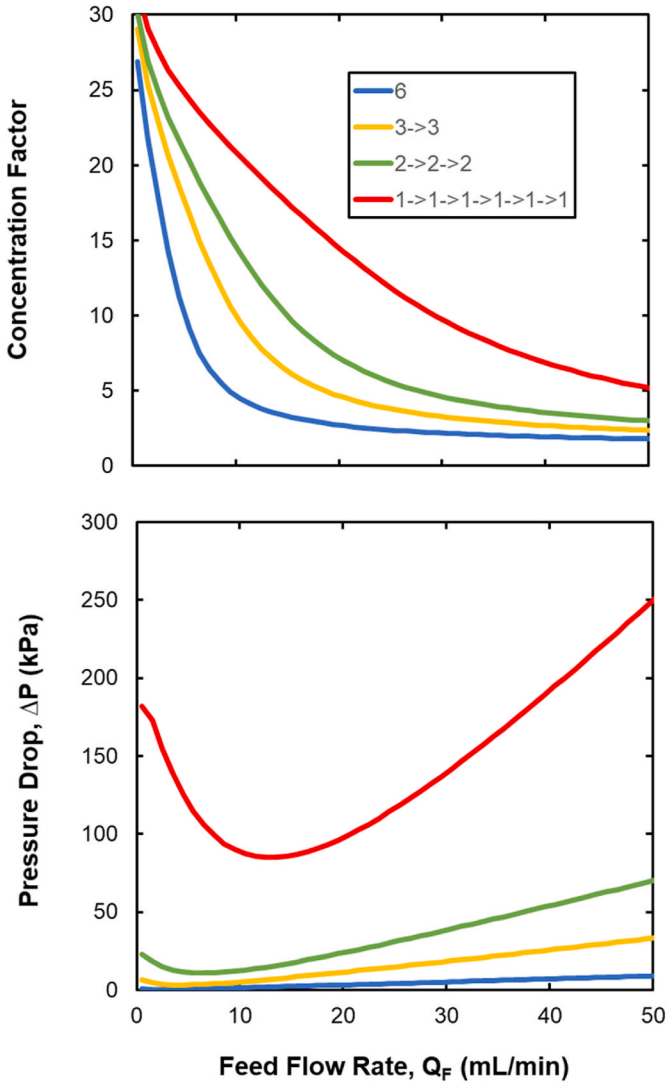

Fig. 4. Concentration factor and pressure drop vs the feed flow rate at $C_F = 10$ g/L for different parallel and series configurations of six channels, each with L = 20 cm and w = 2 cm: (a) 6 channels in parallel, (b) 3 parallel followed by 3 parallel, (c) 2-2-2, and (d) 1-1-1-1-1-1 (all channels in series).

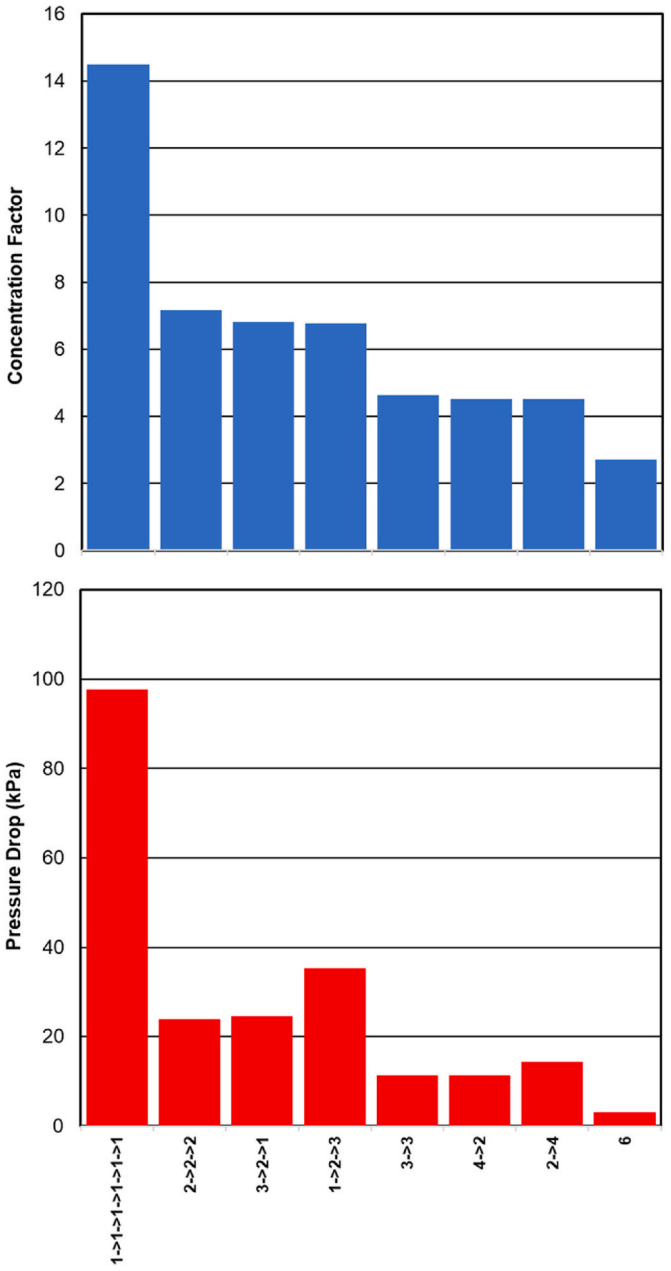

Fig. 5. Effect of module configuration on the concentration factor and pressure drop for $C_F = 10$ g/L and $Q_F = 20$ mL/min.

module configurations at a constant feed flow rate. Since many membranes/modules have a maximum operating pressure, it is also of interest to examine the effect of module configuration at a fixed value of the pressure drop as shown in Fig. 6. In this case, the concentration factor and average filtrate flux are shown for $C_F = 10$ g/L with a feed pressure of 310 kPa (45 psi) and a feed-side pressure drop of 50 kPa. This was done iteratively by guessing a value of Q_F, integrating along the membrane length to evaluate ΔP, and then increasing or decreasing the feed flow rate until ΔP = 50 kPa. Note that it was not possible to find a feed flow rate for the 1-1-1-1-1-1 configuration since the minimum ΔP for this long a module was greater than 50 kPa. Interestingly, the 1-2-3 cascade had the largest concentration factor but with the lowest average filtrate flux since this cascade had to be operated at the lowest feed flow rate ($Q_F = 15$ mL/min) to obtain ΔP = 50 kPa. Thus, the 1-2-3 cascade processes the lowest quantity of mAb solution per unit time. By far the greatest flux was obtained with the 6 in parallel configuration since the short path length (L = 20 cm) and large width (w = 12 cm) allow one to operate at $Q_F = 250$ mL/min, but the concentration factor under these conditions is only 1.2. The configurations with total length of 60 cm have a higher flux but lower concentration factor than those with L = 40 cm since the feed flow rate (at fixed ΔP) varies approximately as $1/L_{total}$.

In this case, the more uniform configurations (2-2-2 and 3-3) have the largest average filtrate flux but the smallest concentration factor.

Most SPTFF processes are designed to achieve a particular concentration factor for a given feed stream, e.g., to concentrate a 10 g/L mAb solution with $Q_F = 20$ mL/min to a final concentration of 20 g/L (corresponding to a 2-fold reduction in flow rate and volume assuming that the membrane is fully retentive to the mAb). In this case, one would like to minimize the membrane area required for this process, which is equivalent to maximizing the filtrate flux. Simulations were performed with SPTFF modules composed of different numbers and configurations of cassettes, with each cassette in a given module having the same length and width to facilitate module assembly. In this case, the width of the channel was fixed at w = 2 cm based on previous results from Jabra et al. [15]. Table 1 shows the required membrane area and the total length, along with the calculated pressure drop, for the different configurations. In each case, the total length and P_F were evaluated iteratively to

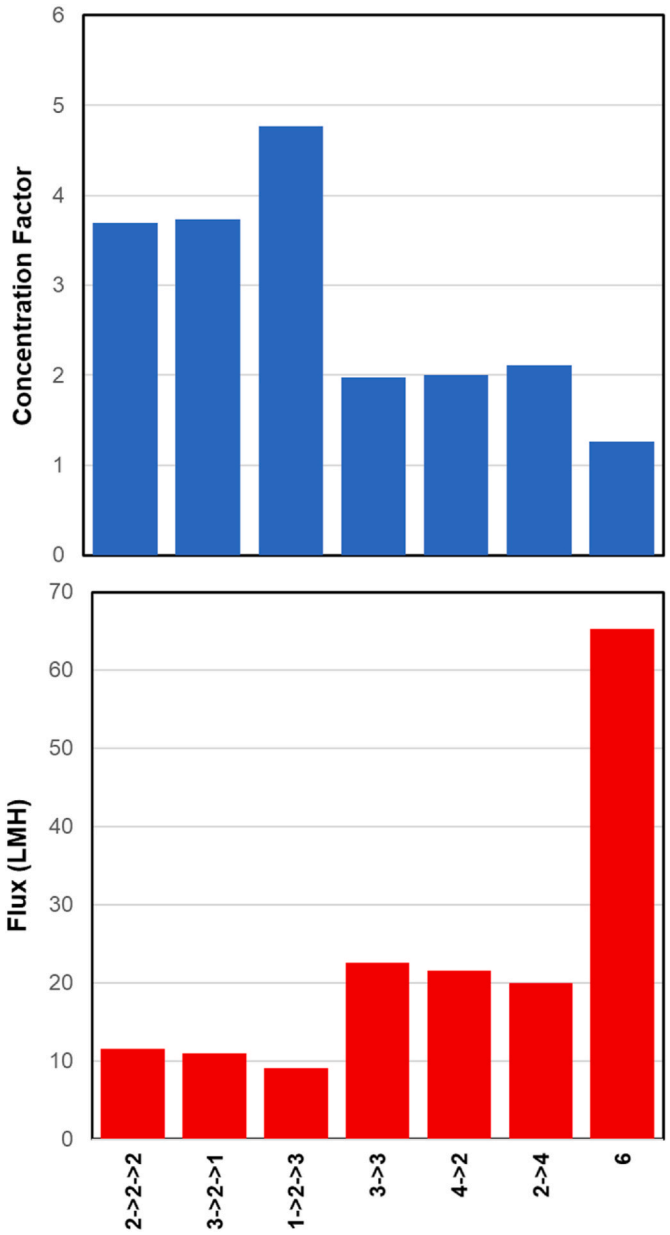

Fig. 6. Effect of module configuration on the concentration factor and average filtrate flux for simulations with $C_F = 10$ g/L, $\Delta P = 50$ kPa, and $P_F = 310$ kPa.

Table 1
Membrane area, total length, and pressure drop to achieve a 2-fold concentration factor for different module configurations with $C_F = 10$ g/L, $Q_F = 20$ mL/min, and exit transmembrane pressure of 14 kPa.

	Membrane area (cm^2)	Total Length (cm)	Pressure Drop (kPa)
1	180	45	46
2	256	32	16
3	312	26	9
2->1	222	37	27
3->2->1	266	33	19
3->2->1->1	241	34	23
4->3->2->1	286	29	14

achieve the desired concentration factor with an exit transmembrane pressure of 14 kPa (2 psi), which was chosen to ensure positive filtration along the entire length of the device. The lowest membrane area is obtained with the module having 1 long channel, although this module also has the largest pressure drop. Using 3 channels in parallel reduces the pressure drop by more than a factor of 5 due to the reduction in total length in combination with the reduction in flow rate per channel (i.e., fluid velocity), with only a 73% increase in membrane area. Just as significantly, the module with the 3-2-1-1 configuration (which is the geometry of the commercial Cadence™ 4-in-series module) provides a 2-fold reduction in pressure drop relative to the single long channel but with less than a 35% increase in membrane area. The optimal trade-off between the membrane area and pressure drop will be determined by the overall process economics, including the cost per unit area for the membrane modules, as well as practical constraints on the pressure drop and the design/assembly of both the individual cassettes and the integrated module.

The calculations in Table 1 are representative of the conditions associated with inline concentration to reduce tankage constraints or to improve the performance of subsequent chromatography steps. SPTFF can also be used for final formulation, but with much higher concentration factors to achieve the desired drug product. Simulations were thus performed for a 20 g/L mAb solution at a feed flow rate of 10 mL/min to achieve a final formulation at 200 g/L, corresponding to a 10-fold concentration factor, as shown in Table 2. The membrane width was w = 3 cm, and the retentate exit pressure was fixed at 35 kPa (5 psi); simulations at lower exit pressures gave similar results except for the long channel where the model did not converge. The somewhat larger membrane width was chosen to reduce the magnitude of the pressure drop given the high mAb concentration in the final formulation. The minimum area is again obtained with a single long channel, although in this case, the pressure drop is so large that the inlet pressure (766 kPa = 111 psi) is well above the maximum operating pressure for currently available membranes/modules (which is typically around 400 kPa). The 3 in parallel configuration again reduces the pressure drop by approximately 5-fold with less than a 2-fold increase in membrane area. However, the 3-2-1-1 staged configuration only reduces the pressure drop by 27% with a 36% increase in membrane area since the pressure drop is determined primarily by the flow of the high viscosity mAb solution near the exit of the module.

4. Conclusion

The growing interest in implementing continuous biomanufacturing processes has led to increased use of SPTFF for debottlenecking existing processes and for developing interconnected and/or continuous processes. This study provided a detailed examination of the design and optimization of SPTFF modules in terms of the channel geometry and module configuration, focusing on the concentration factor, feed-side pressure drop, and required membrane area for a given process objective. The model was in good agreement with experimental data obtained with the Pellicon® SPTFF system using one or two Pellicon® 3 cassettes in series.

The highest concentration factor (at a given feed flow rate) was always obtained using a single long channel, although this configuration led to the highest pressure drop. The pressure drop could be significantly reduced by adding more channels in parallel, which not only reduces the

Table 2
Membrane area, total length, and pressure drop to achieve a 10-fold concentration factor for different module configurations at $C_F = 20$ g/L, $Q_F = 10$ mL/min, and exit transmembrane pressure drop of 35 kPa.

	Membrane area (cm^2)	Total Length (cm)	Pressure Drop (kPa)
1	3100	516	766
2	4390	366	271
3	5360	298	147
2->1	3860	429	591
3->2->1	4480	373	450
3->2->1->1	4210	401	556
4->3->2->1	5040	336	360

flow velocity but also reduces the path length (for the same total membrane area). Alternatively, one can use a staged configuration, with the number of parallel channels varying with position within the module. However, the pressure drop in the staged modules depends strongly on the viscosity of the antibody solution. Although one would intuitively expect the greatest pressure losses to occur near the device inlet due to the high feed flow rate at the entrance to the module, the large increase in viscosity with increasing mAb concentration actually causes a greater pressure drop near the retentate exit under most conditions for the antibody examined in this work. Very different behavior would be seen for a feed in which the viscosity was only a weak function of the mAb concentration.

The modeling approach presented in this paper provides a framework that can be used for the design and optimization of SPTFF modules to achieve specific process objectives, both for inline concentration prior to chromatographic separations and for final formulation (as shown in Tables 1 and 2). This should not only reduce the number of experiments required for the development of SPTFF processes, it should also lead to the development of more productive SPTFF modules (e.g., with lower membrane area) for use in bioprocessing.

CRediT authorship contribution statement

Mario G. Jabra: Data curation, Formal analysis, Investigation, Writing – original draft. **Andrew L. Zydney:** Conceptualization, Funding acquisition, Supervision, Writing – review & editing.

Declaration of competing interest

The authors declare that they have no known competing financial interests or personal relationships that could have appeared to influence the work reported in this paper.

Acknowledgements

The authors would like to acknowledge financial support through the Membrane, Science, Engineering and Technology (MAST) Center, which is funded by grant number 1841474 from the NSF IUCRC program.

Appendix A. Supplementary data

Supplementary data to this article can be found online at https://doi.org/10.1016/j.memsci.2021.120047.

References

[1] J. Dizon-Maspat, J. Bourret, A. D'Agostini, F. Li, Single pass tangential flow filtration to debottleneck downstream processing for therapeutic antibody production, Biotechnol. Bioeng. 109 (4) (2012) 962–970, https://doi.org/10.1002/bit.24377.

[2] T. Elich, E. Goodrich, H. Lutz, U. Mehta, Investigating the combination of single-pass tangential flow filtration and anion exchange chromatography for intensified mAb polishing, Biotechnol. Prog. 35 (5) (2019), e2862, https://doi.org/10.1002/btpr.2862.

[3] A. Brinkmann, S. Elouafiq, J. Pieracci, M. Westoby, Leveraging single-pass tangential flow filtration to enable decoupling of upstream and downstream monoclonal antibody processing, Biotechnol. Prog. 34 (2) (2018), https://doi.org/10.1002/btpr.2601.

[4] C. Perry, A.C.M.E. Rayat, Lentiviral vector bioprocessing, Viruses 13 (2) (2021) 268, https://doi.org/10.3390/v13020268.

[5] C. Casey, T. Gallos, Y. Alekseev, E. Ayturk, S. Pearl, Protein concentration with single-pass tangential flow filtration (SPTFF), J. Membr. Sci. 384 (1–2) (2011) 82–88, https://doi.org/10.1016/j.memsci.2011.09.004.

[6] J. Rucker-Pezzini, L. Arnold, K. Hill-Byrne, T. Sharp, M. Avazhanskiy, C. Forespring, Single pass diafiltration integrated into a fully continuous mAb purification process, Biotechnol. Bioeng. 15 (8) (2018) 1948–1957, https://doi.org/10.1002/bit.26708.

[7] A.M.K. Nambiar, Y. Li, A.L. Zydney, Countercurrent staged diafiltration for formulation of high value proteins, Biotechnol. Bioeng. 115 (1) (2018), https://doi.org/10.1002/bit.26441.

[8] M.G. Jabra, C.J. Yehl, A.L. Zydney, Multistage continuous countercurrent diafiltration for formulation of monoclonal antibodies, Biotechnol. Prog. 115 (1) (2019), https://doi.org/10.1002/btpr.2810.

[9] M. Huter, J. Strube, Model-based optimization of SPTFF ultrafiltration for integration in continuous biopharmaceutical processing, Chemie Ing. Tech. 90 (9) (2018), https://doi.org/10.1002/cite.201855263, 1251-1251.

[10] G. Thakur, A.S. Rathore, Modelling and optimization of single-pass tangential flow ultrafiltration for continuous manufacturing of monoclonal antibodies, Sep. Purif. Technol. 276 (2021) 119341, https://doi.org/10.1016/j.seppur.2021.119341.

[11] G. des los Reyes, L. Mir, Method and apparatus for the filtration of biological solutions, U.S. Patent (2008), 7,384,549 B2.

[12] Application Note Scalability of Cadence Inline Concentrator Modules for Bovine IgG Processing. https://www.pall.com/content/dam/pall/biopharm/lit-library/non-gated/application-notes/14.9534_USD3004_Scalability_Cadence_ILC_Bovine_IgG_AN_EN.pdf. (Accessed 15 October 2021).

[13] MilliporeSigma. Pellicon® Single-Pass Tangential Flow Filtration Versatile Ultrafiltration Technology for Biopharmaceutical Processes Requiring Flexibility, Capacity, and Efficiency. http://www.emdmillipore.com/Web-US-Site/en_CA/-/USD/ShowDocument-Pronet?id=201810.092. (Accessed 15 October 2021).

[14] C.J. Yehl, A.L. Zydney, Single-pass tangential flow filtration using low-cost hollow fiber modules, J. Membr. Sci. 595 (2020), 117517, https://doi.org/10.1016/j.memsci.2019.117517.

[15] M.G. Jabra, A.M. Lipinski, A.L. Zydney, Single pass tangential flow filtration (SPTFF) of monoclonal antibodies: experimental studies and theoretical analysis, J. Membr. Sci. (2021) 637, https://doi.org/10.1016/j.memsci.2021.119606.

[16] M.J. Huter, C. Jensch, J. Strube, Model validation and process design of continuous single pass tangential flow filtration focusing on continuous bioprocessing for high protein concentrations, Processes 7 (11) (2019) 781, https://doi.org/10.3390/pr7110781.

[17] M. Krippl, T. Kargl, M. Duerkop, A. Dürauer, Hybrid modeling reduces experimental effort to predict performance of serial and parallel single-pass tangential flow filtration, Separ. Purif. Technol. 276 (2021), 119277, https://doi.org/10.1016/j.seppur.2021.119277.

[18] E. Binabaji, J. Ma, S. Rao, A.L. Zydney, Theoretical analysis of the ultrafiltration behavior of highly concentrated protein solutions, J. Membr. Sci. 494 (2015) 216–233, https://doi.org/10.1016/j.memsci.2015.07.068.

[19] M. Jabra, A.M. Lipinski, A.L. Zydney, Corrigendum to Single Pass Tangential Flow Filtration (SPTFF) of monoclonal antibodies: Experimental studies and theoretical analysis, J. Membr. Sci. 641 (2022), 119953.

[20] A.R. Da Costa, A.G. Fane, D.E. Wiley, Spacer characterization and pressure drop modelling in spacer-filled channels for ultrafiltration, J. Membr. Sci. 87 (1–2) (1994) 79–98, https://doi.org/10.1016/0376-7388(93)E0076-P.